IEEE Access
Multidisciplinary | Rapid Review | Open Access Journal

Received August 2, 2019, accepted August 11, 2019, date of publication September 11, 2019,
date of current version September 23, 2019.

Digital Object Identifier 10.1109/ACCESS.2019.2940452

Low-Light Image Enhancement Based on Maximal Diffusion Values

WONJUN KIM[1], (Member, IEEE), RYONG LEE[2], MINWOO PARK[2], AND SANG-HWAN LEE[2]
[1]Department of Electrical and Electronics Engineering, Konkuk University, Seoul 05029, South Korea
[2]Research Data Sharing Center, Korea Institute of Science and Technology Information, Daejeon 34141, South Korea

Corresponding author: Ryong Lee (ryonglee@kisti.re.kr)

This work was supported by the Korea Institute of Science and Technology (KISTI), South Korea, through the Research and Development Project, Establishing a System for Sharing and Disseminating Research Data, under Grant K-19-L01-C03.

ABSTRACT A vast amount of pictures are taken every day by using cameras mounted on various mobile devices. Even though the clarity of such acquired images has been significantly improved due to the advance of the image sensor technology, the visual quality is hardly guaranteed under varying illumination conditions. In this paper, a novel yet simple method for low-light image enhancement is proposed via the maximal diffusion value. The key idea of the proposed method is to estimate the illumination component, which is likely to appear as the bright pixel even under the low-light condition, by exploring multiple diffusion spaces. Specifically, the illumination component can be accurately separated from the scene reflectance by selecting the maximal value at each pixel position of those diffusion spaces, and thus independently adjusted for the visual quality enhancement. That is, we propose to adopt the maximal value among diffused intensities at each pixel position, so-called maximal diffusion value, as the illumination component since illumination components buried in the dark tend to be revealed with bright intensities through the iterative diffusion process. In contrast to previous approaches that still pose difficulties to balance between over-saturated and conservative restorations, the proposed method improves the image quality without any significant distortion while successfully suppressing the problem of noise amplification. Experimental results on benchmark datasets show the efficiency and robustness of the proposed method compared to previous approaches introduced in literature.

INDEX TERMS Visual quality, varying illumination condition, low-light image enhancement, maximal diffusion value, multiple diffusion spaces.

I. INTRODUCTION

The low-light condition in everyday photos often occurs due to various environmental factors, e.g., night time, uneven illumination, and structured shadow. This leads to loss of details and surface changes of underlying structures in a given scene, which significantly deteriorate the image quality and degrade the viewing experience. Moreover, such distorted inputs make a dramatic performance drop in many algorithms of computer vision, e.g., object detection [1] and recognition [2], stereo matching [3], etc. Even though the latest mobile devices, especially smartphones, have equipped with camera modules including the relevant solution, it still works under limited situations.

To efficiently improve the visual quality of low-light images, various methods have been developed. In the beginning, many researchers attempted to directly amplify the buried structure to be visible based on the statistical information of the original input image, which can be regarded as the most intuitive and simplest approach for this task. However, relatively bright regions tend to be over-saturated in restoration results of those algorithms and thus the textural features belonging to the corresponding region probably becomes invisible. Histogram equalization and its variants [4], [5] are capable of alleviating this problem by somewhat flattening the distribution of pixel intensities over the whole range. Further, they can be easily combined with several optimization techniques, which give a great help to adaptively adjust the dynamic range by regularizing the histogram of the original image. However, most histogram-based methods only concentrate on improving the contrast without estimating the illumination component in a given scene and thus frequently fail to moderately recover the underlying structure buried in the dark (e.g., under- or

The associate editor coordinating the review of this manuscript and approving it for publication was Sudhakar Radhakrishnan.

over-enhanced in uneven illuminations). On the other hand, the assumption of the Retinex theory [6] that the image can be decomposed into scene reflectance and its illumination has been widely employed for low-light image enhancement. Many studies belonging to this category, i.e., decomposition-based approach, attempted to firstly estimate the illumination component and separate it from the reflectance one, which is directly utilized as the enhanced result in the early stage. Even though textural details are well revealed in the reflectance component, over-highlights of edge-like regions make visually unnatural effects in the enhancement result. Furthermore, defects of halo artifacts around edge structures often occur due to such excessive emphasis.

In this paper, a novel and simple method for low-light image enhancement is proposed. The heart of the proposed method lies on our observation that the bright-light property included in the illumination component is well revealed through the diffusion process even in the dark region. Accordingly, we propose to select the maximal value at each pixel position of multiple diffusion spaces as the illumination component. This scheme is significantly different from previous approaches utilizing the maximal value among RGB channels or the relationship with neighbor pixels for estimating the illumination component, and the corresponding results of illumination estimation are notably different as shown in Fig. 1(c) and (d), for example. It is noteworthy that our pixel-wise pooling operation has a good ability to reduce the blur artifact driven by aggregation in the local window, which has been widely considered for the local consistency of illumination in previous approaches [7], [8]. To avoid the problem of color inconsistency during the enhancement procedure, selecting the maximal diffusion value is only conducted in the intensity channel. Note that the estimated illumination component is adjusted in terms of both global and local stretching schemes as adopted in previous approaches [9], [10]. The main contributions of this paper can be summarized as follows:

- The proposed method attempts to realize the principle that illuminations tend to appear with the bright intensity even in the dark [6], [11]. To this end, we propose to adopt the maximal value at each pixel position of multiple diffusion spaces as the illumination component. By maintaining the maximal value during the diffusion process, the estimated illumination space can be efficiently represented as the piecewise constant form without amplifying unnecessary noise, which still gives difficulties to clearly reveal the illumination space in previous methods, while preserving the underlying structure. This is fairly desirable to achieve the balanced adjustment for the estimated illumination component.
- In contrast to previous approaches that allow for the relationship between color channels or neighbor pixels, the proposed method considers the relationship across diffusion spaces in a pixel-wise manner and thus successfully avoids the problem of color and blur artifacts. This also brings a significant improvement by accurately restoring pixel-level surface details. Moreover, the proposed method does not require any complicated optimization process employed in recent approaches, which is mostly resolved based on the local relationship.

The reminder of this paper is organized as follows. The brief review of previous methods for low-light image enhancement is provided in Section II. The technical details of the proposed method is introduced in Section III. Experimental results on benchmark datasets are demonstrated in Section IV. The conclusions are finally summarized in Section V.

II. RELATED WORK

Since the visual quality of acquired images has a great influence on the performance of various algorithms in computer vision, many researchers have devoted their efforts to improve the visibility regardless of lighting conditions. In this Section, we give a brief review of previous methods for low-light image enhancement.

Most representatively, the histogram equalization [12], which makes the distribution of pixel intensities as flat as possible for improving the dynamic range over the whole image, has been widely employed as a prerequisite for various applications, e.g., object detection and recognition [13]. In particular, its locally-clipped version, called CLAHE [14], provides the outstanding performance by efficiently suppressing over-saturated pixels and thus has been widely employed for enhancing the visual quality of medical images as well as natural ones. On the other hand, several studies attempted to adopt the optimization technique for adaptively adjusting the dynamic range by forcing various regularization effects to the histogram of the original input image. For example, Arici *et al.* [15] conducted adaptive histogram equalization by minimizing a weighted distance between counts of the original histogram and the target one. Celik and Tjahjadi [16] proposed to enhance the contrast by mapping diagonal elements between the 2-D histogram of the original image and its smoothed version, which is obtained by the variational method. Authors of [17] also achieved contrast enhancement by seeking a layered difference in the 2-D histogram constructed via the relationship of neighboring pixels. Raju and Nair [18] proposed to utilize the fuzzy membership to adaptively stretch the dynamic range of intensity values in the original histogram. Apart from this, the quality assessment has been used to derive the optimal histogram mapping for the automatic contrast change [38]. Even though such histogram-based approaches are quite effective to the globally degraded image and computationally efficient, most approaches are vulnerable to nonlinear lighting conditions due to lack of the spatial information.

More recently, inspired by the Retinex theory [6], which tells us a simple principle that the image can be decomposed into two components, i.e., illumination and reflectance, and each pixel value can be represented as a product by those two factors, diverse methods for separating illumination components from a given image have been actively

explored. Specifically, the reflectance, which is often estimated by Gaussian filtering and logarithmic operation both in a single scale [20] and multiple scales [21], has been popularly adopted as the enhancement result without any modification [22], [23]. Even though illumination-invariant features are successfully extracted in the estimated reflectance, the visual unnaturalness (e.g., color inconsistency and over-highlighted edges) often degrades the viewing experience significantly. To resolve this problem, many researchers have begun to focus their attention on stretching the dynamic range of the estimated illumination component and eventually combining it with the separated reflectance for generating the enhancement result. Dong *et al.* [8] proposed to apply the dehazing algorithm, which represents the illumination component as the transition map, to the inverted low-light image. The enhancement result is obtained by inverting the unrealistic estimated result once again. Wang *et al.* [24] attempted to improve the visual quality while keeping the naturalness of a given scene by exploiting the bi-log transformation of the estimated illumination component. Their enhancement results basically provide the visual comfort without over-saturation, however, the phenomenon of the conservative restoration often occurs in our experiments. Fu *et al.* [25] extracted the illumination component by utilizing morphological closing and fused two enhanced illumination maps, which are driven by the sigmoid function and the adaptive histogram equalization. Although their fusing scheme provides the promising enhancement result, it suffers from loss of textural details across multiple scales. To supplement this limitation, they further proposed a weighted variational model for simultaneous reflectance and illumination estimation (SRIE) [26]. Guo *et al.* [27] started with the initial illumination map generated by simply selecting the maximal value among RGB channels. Such initial status is consistently refined by imposing a structural prior in the optimization framework, which is effective to prevent the blur artifact in the enhancement result. The method introduced in [9] proposed to separately handle illumination and reflectance layers by regularizing the color similarity and the spatial smoothness. In [10], the principal energy in a small local region is used as the illumination component, which is simply implemented by applying the orthogonal transform (e.g., singular value decomposition (SVD)) to the intensity lattice.

Even though diverse methods have been steadily studied for low-light image enhancement, they are still struggling to a risk yielding under- or over-enhancement results due to the blindness of illumination structures. Most of recently proposed methods tend to preserve the underlying structure instead of exaggerating color effects, however, it often leads to loss of textural details, e.g., textural features on the surface of objects are smoothed out. Furthermore, several methods require complicated optimization techniques, which are time-consuming on mobile devices. In this paper, a simple and novel method for low-light image enhancement is proposed. Compared to previous approaches, the proposed method concentrates on exploring the brightness property by using the max pooling scheme with multiple diffusion spaces in a pixel-wise manner, which is useful for preventing loss of the textural information. Technical descriptions of the proposed method will be explained in the following Section.

FIGURE 1. (a) Input color image. (b) Intensity channel of (a). (c) Illumination estimated by max-selection among RGB color channels in the local window support. (d) Illumination estimated by the proposed method.

III. PROPOSED METHOD

The principle behind the proposed method is that the illumination component at each pixel position is likely to appear bright even in the dark. In order to robustly extract such "buried" illuminations for low-light image enhancement, we propose to exploit the maximal value obtained from the diffusion process of the intensity channel, which efficiently reveals the illumination structure of a given scene in a piecewise constant manner. In contrast to previous approaches, the proposed method has a good ability to suppress noise as well as blur artifacts by the pixel-wise pooling operation (i.e., selecting the maximal value at each pixel position) on diffusion spaces. The estimated illumination component is adjusted via the global stretching scheme, e.g., conventional Gamma correction, and subsequently combined with the reflectance component, which is estimated according to the Retinex theory. The corresponding result follows by the local refinement for generation of the final enhancement result.

A. ILLUMINATION ESTIMATION USING MAXIMAL DIFFUSION VALUES

Several methods have attempted to extract and represent the bright attribute of the illumination component as introduced above. Most notably, seeking the maximal value of the RGB color channel shows the promising result, which can be simply formulated as follows [25], [27]:

$$L(\boldsymbol{x}) \leftarrow \max_{c\in\{R,G,B\}} I^c(\boldsymbol{x}), \tag{1}$$

where I^c denotes the color channel of a given image and $\boldsymbol{x}$ denotes the pixel position, respectively. Most of such pooling-based improvements essentially require to allow for the local consistency, for example, $L(\boldsymbol{x}) \leftarrow \max_{\boldsymbol{y}\in\Omega(\boldsymbol{x})}\left(\max_{c\in\{R,G,B\}} I^c(\boldsymbol{y})\right)$ where $\Omega(\boldsymbol{x})$ indicates the local patch centered at the pixel position $\boldsymbol{x}$. Even though this scheme efficiently improves the local consistency of the illumination component, aggregation within the local patch often makes the estimation result include unwanted blur and blocky artifacts as shown in Fig. 1(c).

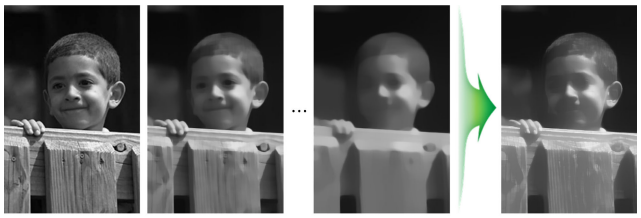

FIGURE 2. (a) Intensity channel of the original image (i.e., $u^0(x)$). (b) $u^3(x)$. (c) $u^{10}(x)$. (d) $L(x)$ computed in (2) (i.e., proposed method).

To cope with this limitation, we propose to exploit the maximal value of multiple diffusion spaces. Since the illumination component is apt to maintain the bright attribute during the diffusion process, our pooling operation across the scale spaces of the intensity channel is expected to successfully reveal the illumination component, which is defined as follows:

$$L(\boldsymbol{x}) \leftarrow u^s(\boldsymbol{x}), \text{ where } s = \max_k \{u^0(\boldsymbol{x}), \ldots, u^P(\boldsymbol{x})\}, \quad (2)$$

where u^k denotes the diffusion space generated with the iteration number of $k \in \{0, 1, \ldots, P\}$. Note that $u^0 = I$ (i.e., no iteration) denotes the intensity channel of the original image. P is the maximal number of iterations, which is set to $P = 10$ in our implementation. An example of the estimated illumination component driven by (2) is shown in Fig. 2. As can be seen, lighting properties are well revealed while preserving the underlying structure (e.g., salient edges) of a given scene. Moreover, the proposed method does not yield blocky artifacts in terms of patch-based operations and thus the scene reflectance can be accurately separated from the given scene without any severe distortion. It should be emphasized again that the piecewise constant result is desirable for illumination estimation since illumination can be regarded as the lighting component and therefore does not contain textural details of a fine scale. In this viewpoint, the diffusion result shown in Fig. 2(b) shows a good performance of edge-aware smoothing, however, fine-scale textural details (e.g., boundaries of eyes and lip) are not suppressed enough. Compared to this, the proposed method yields the piecewise constant result while preserving the boundaries between different surfaces as shown in Fig. 2(d). Therefore, it is thought that the proposed max pooling scheme is more suitable for estimating the illumination space and leads to the reliable performance of image enhancement.

Now, the next task is to construct the diffusion space $u^k(\boldsymbol{x})$ in an efficiency way. To this end, the nonlinear diffusion equation [28], which has been most widely employed in this field, is adopted as follows:

$$u^{k+1}(\boldsymbol{x}) = u^k(\boldsymbol{x}) + \Delta\tau \operatorname{div}\left(g(|\nabla u^k(\boldsymbol{x})|)\nabla u^k(\boldsymbol{x})\right), \quad (3)$$

where g is the conductance function for controlling the diffusivity and $\Delta\tau$ denotes the time step, i.e., evolution rate. In our implementation, the total iteration number is adaptively determined by considering the contextual information of a given scene. More specifically, it is thought that the nonlinear diffusion is converged when the difference between diffusion spaces becomes sufficiently small, which can be formulated as follows: $c = \frac{1}{HW}\sum_{\boldsymbol{x}} |u^k(\boldsymbol{x}) - u^{k-1}(\boldsymbol{x})|$ where H and W denote height and width of the input image, respectively, and the diffusion process stops when $c < 1.0$ for the proposed method. Note that the maximal number of iterations is limited to 10 (i.e., $P = 10$) as introduced. The original diffusion model in (3) provides quite reliable results for selective smoothing, however, it is theoretically ill-posed [29], [30], i.e., it cannot discriminate textural edges, which need to be smoothed out during the diffusion process, from salient ones (e.g., object boundaries). Therefore, this property gives a difficulty to simultaneously satisfy both conditions, i.e., suppression of textural edges and preservation of surface boundaries, which is highly required for our illumination estimation. To resolve this problem, the total variation flow [31] is employed for the conductance function in the proposed method, which is simply computed as follows:

$$g(|\nabla u|) = \frac{1}{|\nabla u| + \epsilon}, \quad (4)$$

where ϵ is a small positive number to avoid the problem of zero gradients. According to the property of the total variation flow, relatively small-scale elements in the intensity channel are efficiently smoothed out while preserving the boundary across different structures [32]. This is fairly desirable for excluding textural features on the surface from the illumination component as shown in Fig. 2(d).

In general, the nonlinear diffusion of (3) has been solved in a numerical manner, which requires quite a lot iterations with the small time step for the stability. To alleviate this hard constraint, the additive splitting operator (AOS) scheme [33] can be regarded as a good alternative due to its semi-implicit nature. That is, the AOS scheme guarantees the stability of the diffusion process even with the arbitrary large value for the time step $\Delta\tau$. The original version of the nonlinear diffusion can be reformulated with the AOS scheme as follows:

$$u^{k+1}(\boldsymbol{x}) = \frac{1}{2}\sum_{d\in\{x,y\}} \left(I(\boldsymbol{x}) - 2\Delta\tau A_d\left(u^k(\boldsymbol{x})\right)\right)^{-1} u^k(\boldsymbol{x}), \quad (5)$$

where A_d is a diffusive matrix whose elements are related to derivatives with respect to horizontal ($x \leftarrow d$) and vertical ($y \leftarrow d$) directions, respectively. For more details about the diffusive matrix, see [33]. $\Delta\tau$ denotes the time step as mentioned above, and it now can be set to the relatively large value, e.g., $\Delta\tau = 10.0$, for the fast operation.

In summary, the intensity channel of the input image is diffused by utilizing the AOS scheme with the adaptive stopping criteria (i.e., $c < 1.0$), and the maximal value at each pixel position is selected during this diffusion process for estimating the illumination component.

Algorithm 1 Low-Light Image Enhancement Based on Maximal Diffusion Values

Data: I: intensity channel of the input color image
$\boldsymbol{x} = (x, y)$: pixel position
H : height, W : width
Result: Enhanced color image
while $1 \le x \le W$ *and* $1 \le y \le H$ **do**
1. Illumination estimation
i) Compute the diffusion space $u^k(\boldsymbol{x})$ via AOS
ii) Select the maximal diffusion value at each pixel position as the illumination component
: $L(\boldsymbol{x}) \leftarrow u^s(\boldsymbol{x}),\ s = \max_k\{u^0(\boldsymbol{x}), \ldots, u^P(\boldsymbol{x})\}$
: Use the adaptive stopping criteria
2. Image enhancement
iii) Apply the Gamma function to $L(\boldsymbol{x})$ (see (ii))
: $\tilde{L}(\boldsymbol{x}) = 255 \times \left(\frac{L(\boldsymbol{x})}{Z}\right)^{1/\gamma}$
iv) Restore the intensity $\tilde{I}(\boldsymbol{x}) = \tilde{L}(\boldsymbol{x}) \times R(\boldsymbol{x})$
$\boldsymbol{x} = (x, y)$ increases in a raster scanning manner
end
⋆ Final step : CLAHE is applied to $\tilde{I}(\boldsymbol{x})$
⋆ For the color image, conduct HSV→RGB conversion with the restored intensity (obtained from final step)

B. IMAGE ENHANCEMENT

According to the Retinex theory, the scene reflectance can be easily extracted from a given scene as follows:

$$R(\boldsymbol{x}) = \frac{I(\boldsymbol{x})}{L(\boldsymbol{x}) + \epsilon}, \tag{6}$$

where $I(\boldsymbol{x})$ and $L(\boldsymbol{x})$ denote the intensity channel and the estimated illumination by using (2), respectively. ϵ is the small positive number to avoid the zero division as mentioned. An example of the reflectance estimation $R(\boldsymbol{x})$ is shown in Fig. 3(c). As can be seen, underlying structures, for example, shaded eyes of a boy, are well revealed in the scene reflectance. On the other hand, the estimated illumination is now ready to be adjusted for improving the visual quality of the original low-light image. Similar to previous methods, we first apply the Gamma function to stretch the dynamic range in a global sense as follows:

$$\tilde{L}(\boldsymbol{x}) = 255 \times \left(\frac{L(\boldsymbol{x})}{Z}\right)^{1/\gamma}, \tag{7}$$

where Z is a scaling factor that makes the result to be the form of an image, which is set to 5.0 in our implementation. γ is also set to the conventional level, i.e., $\gamma = 2.2$. After that, the intensity image is newly restored by a product of illumination and reflectance components at each pixel position as follows:

$$\tilde{I}(\boldsymbol{x}) = \tilde{L}(\boldsymbol{x}) \times R(\boldsymbol{x}). \tag{8}$$

To allow for the local adjustment as well as global stretching conducted in (7), the CLAHE [14] method is applied to the restored intensity image for the final result, which is shown in Fig. 3(d). It is noteworthy that nonuniformly lighted regions are successfully adjusted without yielding the over-saturated effect. Finally, the enhanced color image can be obtained from the conversion of HSV→RGB via our restored intensity channel shown in Fig. 3(d). The comparison of the visual quality between the original input and the enhancement result by the proposed method is provided in Fig. 4. The shaded eye in the original image (see ①) is successfully restored in the enhancement result and the surface details are clearly revealed as well (see ②) due to the balanced lighting effect. Along with low-light images, the hyper-reflective effects often occur in daily-life photos. Even though the key idea of the proposed method, i.e., the concept of the maximal diffusion value, for estimating illumination components from a given scene is still valid for such high-light conditions, the other procedures need to be additionally refined and optimized to achieve the best performance for high-light conditions, which are beyond the scope of this paper.

For the sake of completeness, the summary of the proposed method is shown in Algorithm 1.

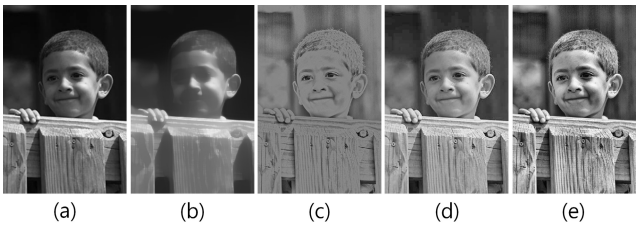

FIGURE 3. (a) Intensity channel of the original image. (b) Estimated illumination. (c) Estimated reflectance. (d) Adjustment result by the Gamma function. (e) Final enhancement result for the intensity channel of the original image.

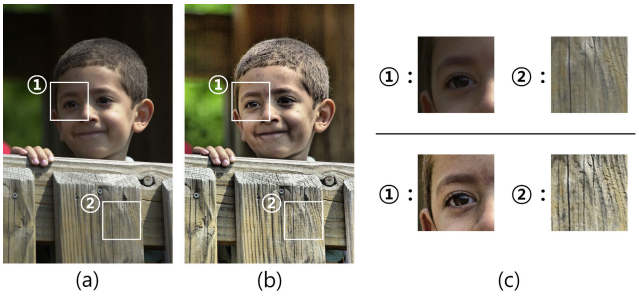

FIGURE 4. (a) Original color image. (b) Enhancement result by the proposed method. (c) Enlarged regions from (a) and (b). Note that the effect of uneven lighting is moderately adjusted without color distortions and over-saturation in the result of the proposed method.

IV. EXPERIMENTAL RESULTS

In this Section, various experimental results are demonstrated based on two benchmark datasets, i.e., NASA [34] and HDR [35] datasets, which have been most widely employed for the performance evaluation of low-light image enhancement. The samples from the NASA dataset (25 images) contain various low-light conditions, e.g., backlighting, casting shadows, cloudy weather, etc., while those of the HDR dataset

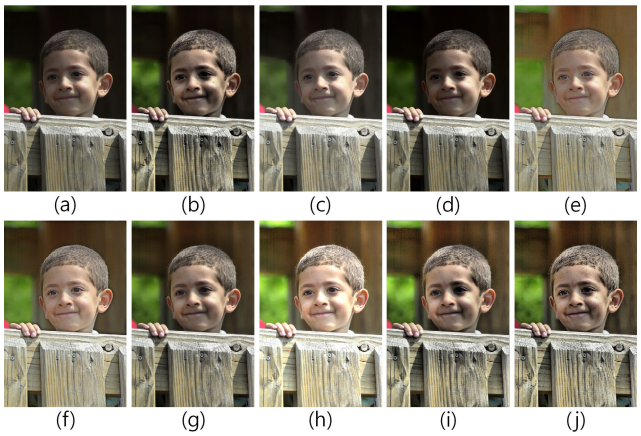

FIGURE 5. Low-light image and its enhancement results by various methods. (a) Original input image. (b) CLAHE [14]. (c) CVC [16]. (d) LDR [17]. (e) NPEA [24]. (f) SRIE [26]. (g) FUN [36]. (h) LIME [27]. (i) PPEA [10]. (j) Proposed method.

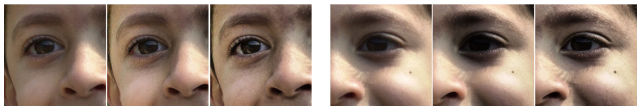

FIGURE 6. Enlarged regions of enhancement results by FUN [36], PPEA [10], and the proposed method (from left to right) in each sub-figure. Note that textural details are well revealed even in the dark by the proposed enhancement scheme.

(seven images) are mostly acquired under backlighting environments. The sizes of images are generally set to 2000×1312 (or 1312×2000) pixels and 1350×900 (or 900×1350) pixels in NASA and HDR datasets, respectively. Details of experiments will be explained in the following subsections.

A. QUALITATIVE ANALYSIS

For the performance comparison, we employ some representative methods for low-light image enhancement, which are CLAHE [14], CVC [16], LDR [17], NPEA [24], SRIE [26], FUN [36], LIME [27], and PPEA [10]. First of all, enhancement results for the previous sample provided in Fig. 1(a) are shown in Fig. 5. Specifically, several methods, e.g., CLAHE, CVC, and LDR, show somewhat conservative results whereas attribute and saturation of the original color are pretty changed in NPEA and SRIE methods. Even though FUN yields the moderately enhanced result, textural details are relatively less restored compared to PPEA and the proposed method. In the result of CLAHE and PPEA, the shaded area is adversely emphasized, for example, the left eye of a boy. Note that LIME shows the visually impressive result, however, it still suffers from the over-saturation problem. In contrast to previous approaches, the proposed method has a good ability to successfully stretch the dynamic range of low-lighted regions while revealing the surface details as well. To support the corresponding analysis, some enlarged regions from the enhancement results are compared in Fig. 6. As can be seen, the shape of iris, which is buried in the dark of the original input, is most accurately revealed in the result of the proposed method (see the rightmost image), and textural details are clearly restored as well.

Comparison results based on the NASA dataset whose samples are acquired under various low-light environments are shown in Fig. 7. Overall, results by the proposed method are reliably restored without under- or over-enhancement, and efficiently highlight textural details as well as local contrast compared to previous approaches. More concretely, CLAHE, CVC, and LDR tend to conduct conservative restoration while LIME shows some results of over-enhancement, e.g., the second and the fifth rows in Fig. 7(h). In particular, the last row of Fig. 7 shows an example of the medical image, which is generally captured under the skin (i.e., very low-light condition with the existence of light scattering). Most previous approaches fail to accurately represent textural details buried in the dark of the mammography image, for example, SRIE and FUN yield the low contrast whereas the result by LIME is extremely over-saturated. In contrast, PPEA and the proposed method provide quite a good enhancement result, which efficiently reveal textural details while keeping the relative contrast as well. To show details of the difference between enhancement results by previous models and the proposed method, enlarged regions of several samples are shown in Fig. 10. Specifically, the contrast of the picture in the T-shirt is successfully improved by the proposed method, which gives better viewing experience to users. In the second example, facial structures are clearly restored with relatively high contrast in the result of the proposed method. Moreover, surface textures, which belong to the bright area (see the white rectangle in the bottom), are well preserved during the enhancement procedure without over-saturation compared to previous approaches. More examples of enhancement results by the proposed method are shown in Figs. 8 and 9. It can be seen that the proposed method yields good overall results, and improves the image quality successfully even under the low-light environment in terms of the existence of the haze as shown in the last example of Fig. 8.

In the following, enhancement results for the HDR dataset are also shown in Fig. 11. First of all, most samples from the HDR dataset are taken under the backlight condition and thus the image is globally dark. In this case, LIME shows the visually impressive results, however, it sometimes fails to make a balance of the contrast in foreground and background, for example, the tree outside the window is over-saturated in the first sample, whereas LDR shows the result of the under-enhancement. NPEA and SRIE yield loss of surface details with slight distortions of color attributes as shown in Fig. 11(e) and (f). Compared to previous approaches, the proposed method moderately improves the contrast while efficiently revealing textural details on the surface. To highlight the difference between the performance of PPEA and the proposed method, enhancement results for several local regions, which are obtained from Figs.7 and 11, are shown in Fig. 12. As can be seen, the proposed method efficiently restores details of textures while maintaining the high contrast

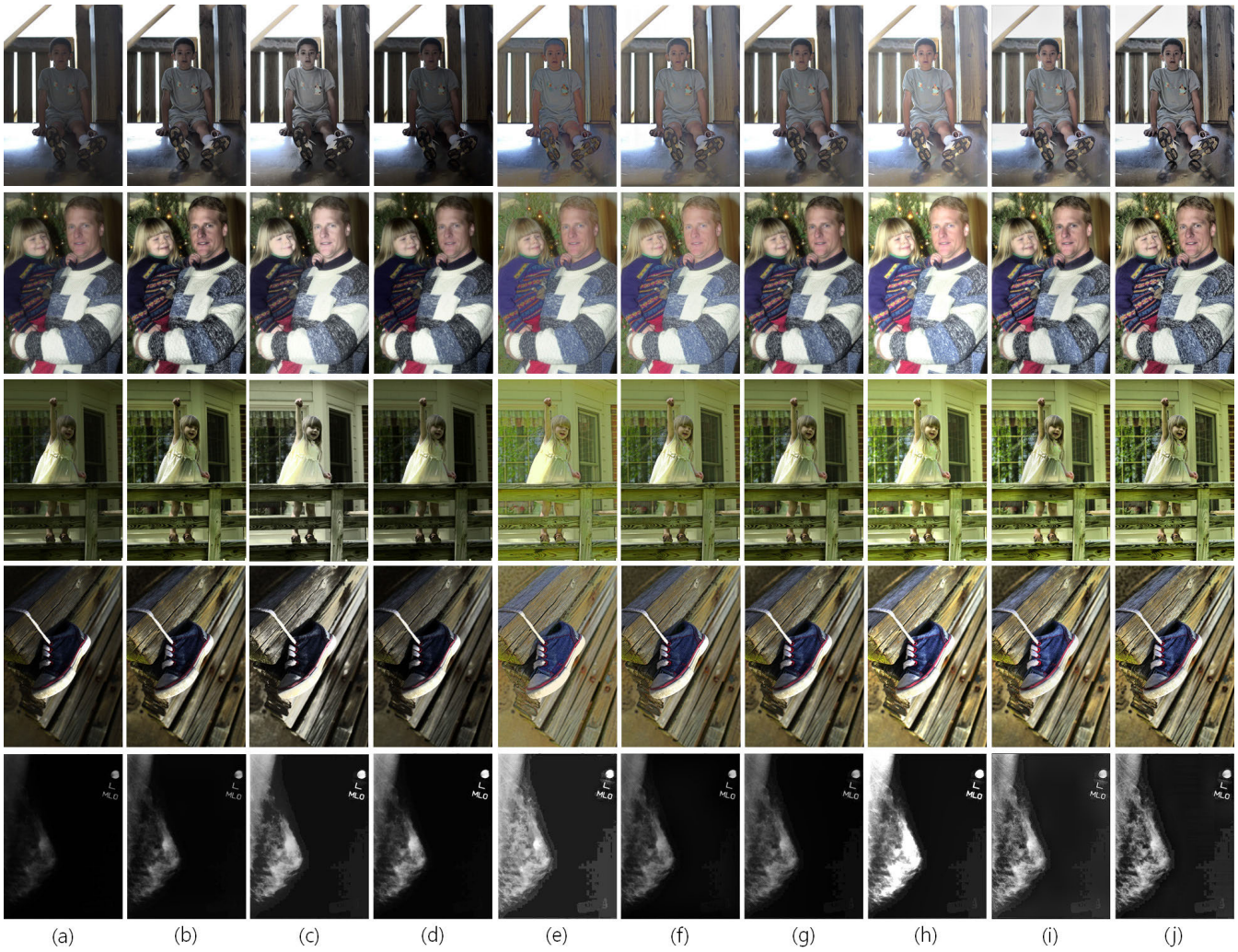

FIGURE 7. (a) Test samples from the NASA dataset. Enhancement results of test samples in the NASA dataset by (b) CLAHE [14], (c) CVC [16], (d) LDR [17], (e) NPEA [24], (f) SRIE [26], (g) FUN [36], (h) LIME [27], (i) PPEA [10], and (j) the proposed method.

FIGURE 8. More enhancement results for the NASA dataset by the proposed method. Top : original input images. Bottom : enhancement results by the proposed method.

compared to PPEA. In addition, more enhancement results for images acquired by the smartphone under various real-world scenarios are shown in Fig. 13. It is noteworthy that the proposed method provides visually comfortable results without any significant distortion both in the color attribute and the contrast. However, the proposed method sometimes yields halo artifacts around strong edges on the flat background, e.g., second example in Fig. 8 and fourth example

TABLE 1. Performance comparison using the NASA dataset (concerning each metric, the best results are shown in bold).

Methods	Input	CLAHE [14]	CVC [16]	LDR [17]	NPEA [24]	SRIE [26]	FUN [37]	LIME [27]	PPEA [10]	Ours
NIQE (↓)	5.106	4.161	3.873	4.458	3.755	4.108	4.201	4.018	4.512	**3.672**
BTMQI (↓)	4.763	3.809	4.393	4.527	3.466	3.508	3.527	4.549	3.537	**3.375**
NIQMC (↑)	4.625	5.057	**5.437**	5.129	4.709	4.809	4.962	5.097	5.287	5.406
C-PCQI (↑)	-	1.132	1.032	1.039	0.955	0.960	1.098	0.955	1.110	**1.189**

TABLE 2. Performance comparison using the HDR dataset (concerning each metric, the best results are shown in bold).

Methods	Input	CLAHE [14]	CVC [16]	LDR [17]	NPEA [24]	SRIE [26]	FUN [37]	LIME [27]	PPEA [10]	Ours
NIQE (↓)	4.653	3.622	3.917	4.326	3.536	3.958	3.799	3.582	3.212	**3.195**
BTMQI (↓)	5.943	3.872	5.982	5.541	4.106	3.197	3.082	4.618	**2.671**	3.068
NIQMC (↑)	4.685	5.058	5.258	4.952	4.370	4.989	4.927	5.027	5.273	**5.394**
C-PCQI (↑)	-	1.122	1.007	1.014	0.883	0.963	1.049	0.918	1.053	**1.134**

FIGURE 9. More enhancement results for the NASA dataset by the proposed method. Top : original input images. Bottom : enhancement results by the proposed method. Note that the proposed method works well even under various lighting conditions, e.g., structured shadows and uneven lighting.

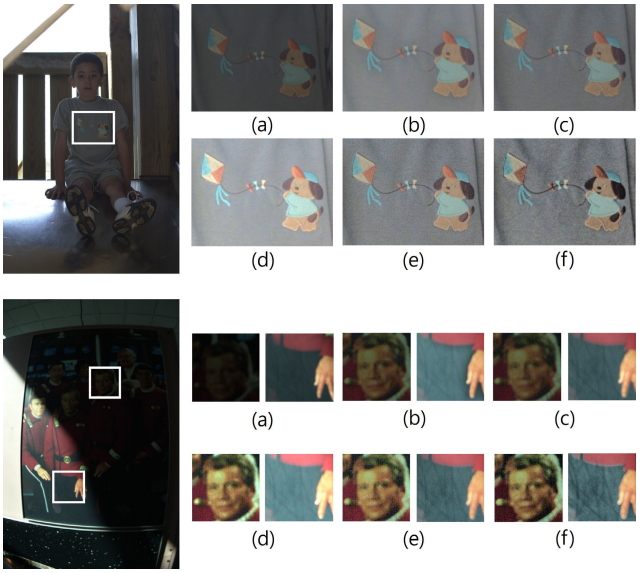

FIGURE 10. Performance comparison in several local regions (white rectangles). (a) Original input. (b) SRIE [26]. (c) FUN [36]. (d) LIME [27]. (e) PPEA [10]. (f) Proposed method.

in Fig. 13. This is because the reflectance (i.e., textural surface) is computed by dividing the original intensity image with the piecewise constant illumination space, which is estimated by using our maximal diffusion values, according to the Retinex theory. Therefore, small-scale components (e.g., strong edges or highly textured regions), which make relatively large changes of pixel values during the diffusion process, tend to be excessively emphasized in the enhancement result. This probably leads to the performance drop even though the proposed method successfully suppresses such artifacts in most cases.

B. QUANTITATIVE ANALYSIS

To compare the enhancement performance quantitatively, the visual quality metric (VQM) has been popularly employed in literature. In our experiments, we also adopt four representative VQMs, which are NIQE [37], BTMQI [38], NIQMC [39], and C-PCQI [40]. The first three metrics are defined in a no-reference manner, i.e., they do not require distortion-free images (ground truth) whereas the last one is based on the full-reference scheme, utilizing the difference between the ground truth and the input image. Specifically, NIQE [37] works based on the quality-aware collection of the natural scene statistics (NSS) model, which enables to provide the perceptual quality of a given image. The performance of color tone mapping can be measured by BTMQI [38] while the difference of the color attribute between the original input and the enhancement result is efficiently estimated by using the C-PCQI [40] metric. NIQMC [39] computes the entropy for informative areas predicted by visual saliency and combines local and global properties to estimate the image quality. It is noteworthy that such VQMs are useful to evaluate the performance of image enhancement at various viewpoints. The results of the performance evaluation in each dataset are shown in Table 1 and 2, respectively. Note that lower values are more desirable in NIQE and BTMQI metrics whereas the higher values indicate the better performance in NIQMC and C-PCQI. As shown in Table 1, the proposed method is able to provide the visually acceptable result even with diverse low-light conditions in the NASA dataset. Regarding the backlight environment mostly contained in the HDR dataset, color

TABLE 3. Performance comparison with standard image datasets, i.e., ISO12640-2 [41], Canon [42], and Kodak [43] datasets.

Results for the ISO12640-2 dataset										
Methods	Input	CLAHE [14]	CVC [16]	LDR [17]	NPEA [24]	SRIE [26]	FUN [37]	LIME [27]	PPEA [10]	Ours
NIQE (↓)	7.483	6.375	7.363	7.561	6.471	5.699	6.561	7.147	6.367	5.609
BTMQI (↓)	4.937	4.879	4.728	4.723	4.664	4.529	4.571	5.142	4.687	4.951
NIQMC (↑)	4.987	5.347	5.326	5.291	4.722	5.273	5.202	5.237	5.535	5.375
C-PCQI (↑)	-	1.031	0.982	1.009	0.966	0.965	1.019	0.946	0.988	1.061
Results for the Canon dataset										
Methods	Input	CLAHE [14]	CVC [16]	LDR [17]	NPEA [24]	SRIE [26]	FUN [37]	LIME [27]	PPEA [10]	Ours
NIQE (↓)	4.971	4.597	4.495	4.691	4.509	4.551	4.646	4.481	5.492	4.874
BTMQI (↓)	3.441	3.396	3.228	3.186	3.211	3.293	2.977	4.923	3.786	3.862
NIQMC (↑)	5.121	5.517	5.675	5.638	5.109	5.279	5.291	5.398	5.437	5.497
C-PCQI (↑)	-	1.151	1.027	1.032	0.958	0.956	1.091	0.963	1.087	1.206
Results for the Kodak lossless dataset										
Methods	Input	CLAHE [14]	CVC [16]	LDR [17]	NPEA [24]	SRIE [26]	FUN [37]	LIME [27]	PPEA [10]	Ours
NIQE (↓)	3.019	3.329	3.075	3.026	3.048	2.858	3.324	3.093	4.539	3.654
BTMQI (↓)	3.577	4.289	4.092	3.736	3.977	4.401	3.722	5.853	4.292	4.429
NIQMC (↑)	4.981	5.566	5.548	5.543	4.927	5.055	5.179	5.101	5.336	5.453
C-PCQI (↑)	-	1.233	1.078	1.086	0.968	0.939	1.134	0.927	1.203	1.261

FIGURE 11. (a) Test samples from the HDR dataset. Enhancement results of test samples in the HDR dataset by (b) CLAHE [14], (c) CVC [16], (d) LDR [17], (e) NPEA [24], (f) SRIE [26], (g) FUN [36], (h) LIME [27], (i) PPEA [10], and (j) the proposed method.

attributes and textures are well preserved in the enhancement result of the proposed method compared to previous models as shown in Table 2. Therefore, it is thought that the proposed method is fairly desirable to be applied for diverse applications, which require the high-visibility in the dark. For more detailed analysis, metric values for all the samples from both datasets are also shown in Fig. 14. Note that the image index follows that of the original dataset. Based on this, we analyzed the performance drop of the proposed method occurring in NIQMC or BTMQI metrics. Specifically, highly textured areas in the eighth image (see Fig. 15(a)) of the NASA dataset are excessively emphasized by the proposed method, which probably leads to the performance drop of the NIQMC value compared to approaches yielding the conservative restoration. Since the NIQMC metric takes account the maximum-information region for estimating the visual quality, distortions of such textured regions give negative effects to calculate a score. That is the reason why the proposed method shows the lower performance compared to CVC for the NIQMC metric. On the other hand, the BTMQI values of the proposed method are mostly higher than those of PPEA for samples from the HDR dataset. This is because the color tends to slightly darken compared to those of PPEA (see Fig. 15(b)) even though the structural information (e.g., edges and textures) is efficiently restored with high contrast in the result of the proposed method.

Furthermore, experimental results on the standard image datasets, i.e., ISO12640-2 [41] (15 images), Canon [42]

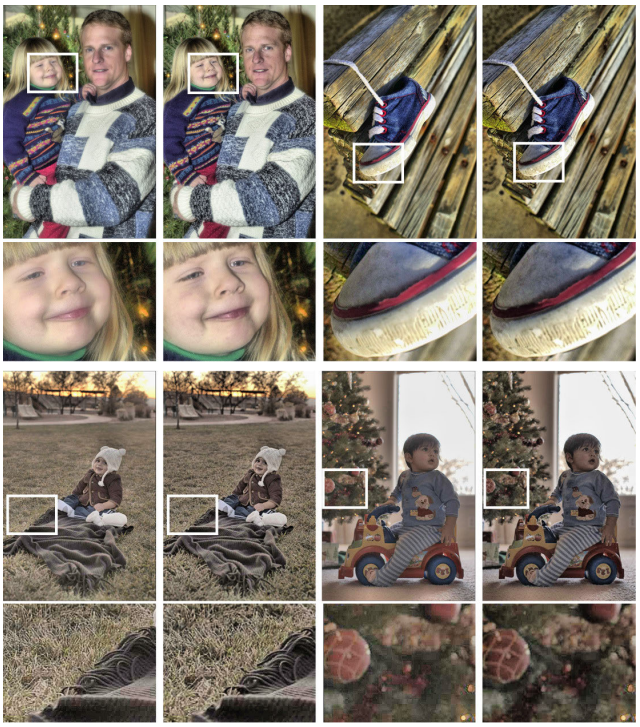

FIGURE 12. Detailed comparison between enhancement results of PPEA and the proposed method. Odd columns : results by PPEA. Even columns : results by the proposed method. Note that details of textures and high contrast are well revealed in results of the proposed method.

FIGURE 13. More enhancement results for images taken by the smartphone. Top : original captured images. Bottom : enhancement results by the proposed method.

(18 images), and Kodak lossless [43] (24 images) datasets, also have been provided in Table 3. Specifically, all the methods employed for our experiments are devised to particularly improve the visibility of low-light images, and thus the performance of the certain method is not dominant for standard images, i.e., images acquired under the normal lighting condition. Since methods conducting conservative restorations for low-light images, e.g., CVC and LDR, do not make significant changes, they provide relatively stable performance in normal environments. Note that the proposed method consistently shows a good ability to preserve the color attribute (see results of the C-PCQI metric). Some enhancement

TABLE 4. Performance comparison with tone-mapping methods.

Results for the NASA dataset				
Methods	NIQE (↓)	BTMQI (↓)	NIQMC (↑)	C-PCQI (↑)
MST [46]	4.216	5.059	3.597	0.781
CRM [47]	4.131	4.469	4.696	0.912
LD [48]	3.564	3.788	5.251	0.953
Ours	3.672	3.375	5.406	1.189
Results for the HDR dataset				
Methods	NIQE (↓)	BTMQI (↓)	NIQMC (↑)	C-PCQI (↑)
MST [46]	4.152	5.945	3.458	0.734
CRM [47]	3.763	5.745	4.574	0.861
LD [48]	3.447	3.029	5.543	0.985
Ours	3.195	3.068	5.394	1.134

TABLE 5. Performance variations according to parameter settings for the NASA dataset.

Methods	NIQE (↓)	BTMQI (↓)	NIQMC (↑)	C-PCQI (↑)
$c = 0.5$	3.696	3.331	5.381	1.191
$c = 1.0$	3.672	3.375	5.406	1.189
$c = 1.5$	3.689	3.268	5.341	1.189
$\Delta t = 5.0$	3.679	3.351	5.398	1.189
$\Delta t = 10.0$	3.672	3.375	5.406	1.189
$\Delta t = 15.0$	3.676	3.371	5.401	1.189

TABLE 6. Performance variations according to parameter settings for the HDR dataset.

Methods	NIQE (↓)	BTMQI (↓)	NIQMC (↑)	C-PCQI (↑)
$c = 0.5$	3.226	3.038	5.358	1.134
$c = 1.0$	3.195	3.068	5.394	1.134
$c = 1.5$	3.083	2.956	5.300	1.132
$\Delta t = 5.0$	3.206	3.028	5.378	1.133
$\Delta t = 10.0$	3.195	3.068	5.394	1.134
$\Delta t = 15.0$	3.204	3.116	5.394	1.134

results by the proposed method for these datasets are shown in Fig. 16.

The proposed method is further compared with tone-mapping methods, which also improve the visibility of low-light images efficiently by reproducing the standard dynamic range while preserving the visual information. To do this, we employed three tone-mapping methods, i.e., MST [45], CRM [46], and LD [47], and the comparison results are shown in Table 4 and Fig. 17, respectively. As can be seen, models, which are based on the multiscale decomposition via edge-aware smoothing [45] and the camera response [46], basically restore the structural information as well as color attributes from low-light conditions, however, they are apt to yield hazy-like results as shown in Fig. 17(b) and (c). In particular, the layer decomposition-based approach [47] shows a good performance in the metric considering tone mapping, i.e., BTMQI. From Table 4 and Fig. 17, it is thought that the proposed method still provides the competitive performance for low-light image enhancement compared to tone-mapping approaches.

For optimization of the proposed method, the performance according to various parameter settings is also evaluated.

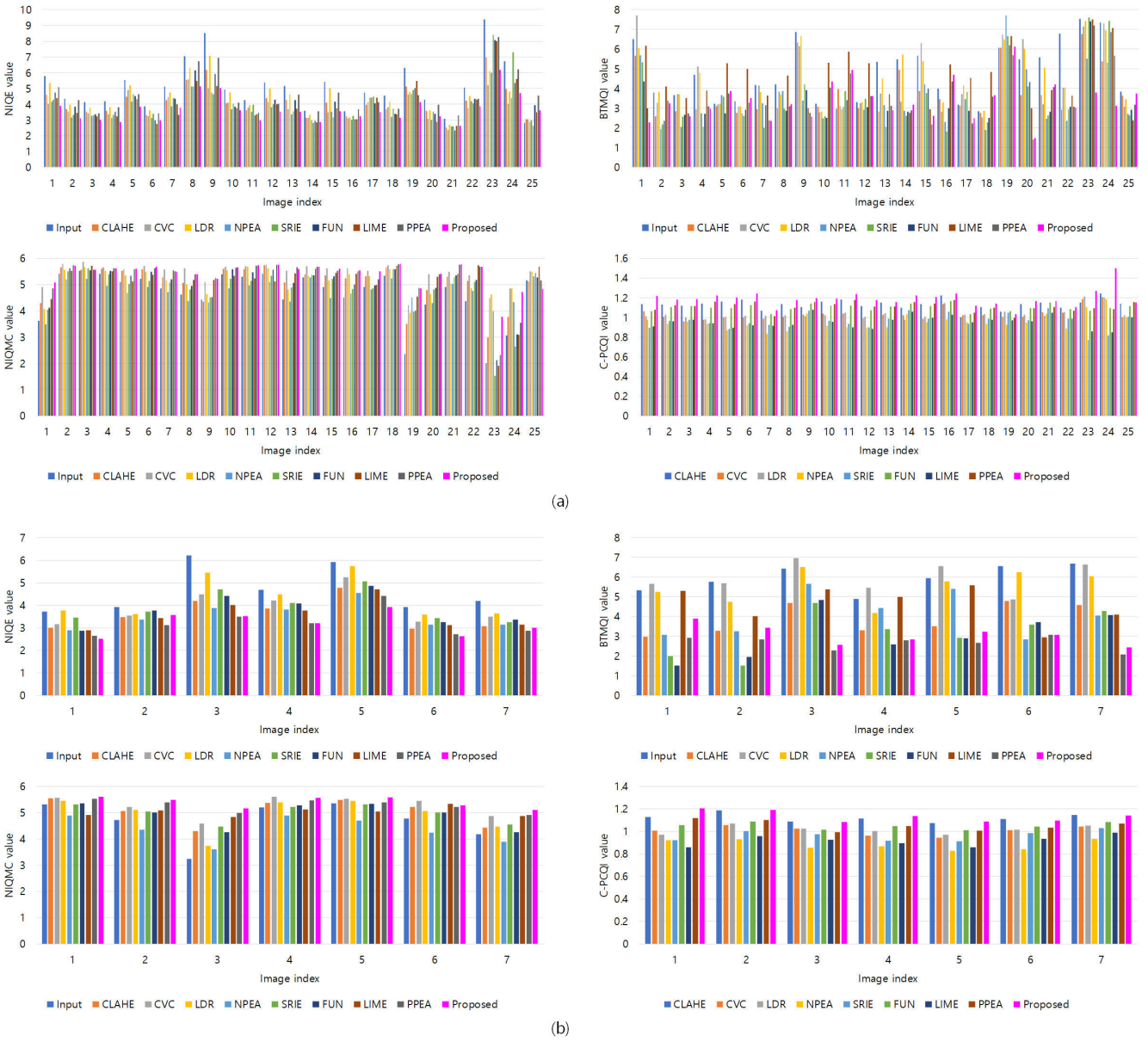

FIGURE 14. (a) Metric values for all the samples (25 images) from the NASA dataset. (b) Metric values for all the samples (seven images) from the HDR dataset. Best view in colors.

TABLE 7. Comparison of the average processing time (Matlab) in NASA and HDR datasets.

Methods	CLAHE [14]	CVC [16]	LDR [17]	NPEA [24]	SRIE [26]	FUN [37]	LIME [27]	PPEA [10]	Ours
NASA	0.22 sec	4.11 sec	1.23 sec	87.75 sec	64.29 sec	2.58 sec	1.74 sec	27.68 sec	15.84 sec
HDR	0.17 sec	2.07 sec	0.68 sec	44.29 sec	39.77 sec	1.44 sec	0.87 sec	13.27 sec	7.31 sec

Specifically, two main parameters, i.e., the stopping criteria c and the time step Δt for the nonlinear diffusion, are tuned to achieve the best performance as shown in Table 5 and 6, respectively. In particular, the performance for the BTMQI metric is significantly improved when the threshold value for stopping the diffusion process is set to 1.5. The overall performance is relatively stable with various setting conditions of the time step. For more improvement, the parameter of Gamma correction, i.e., γ, also can be tuned and we checked that the performance for the NIQMC metric is successfully improved (e.g., 5.394 $\rightarrow$ 5.417 for the HDR dataset) without the significant performance drop for other metrics when γ is set to 3.2. Note that the default setting is given as $c = 1.0$ and $\Delta t = 10.0$, and a parameter is fixed as the default value when the other one is in the test.

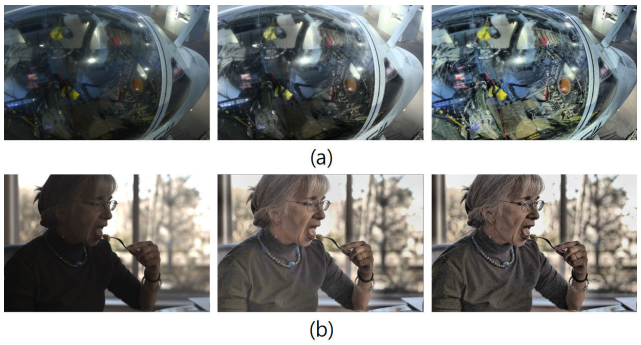

FIGURE 15. Examples of the performance drop in the proposed method. (a) Excessively highlighted textures (left : input, middle : CVC, right : ours). (b) Darken colors (left : input, middle : PPEA, right : ours).

FIGURE 16. Top : original input images. Bottom : enhancement results by the proposed method. From left to right : samples from ISO [41], Canon [42], and Kodak lossless [43] dataset.

The comparison of the average processing speed is also shown in Table 7. All the methods are run on a single PC with Intel Xeon 2.2GHz CPU and 64 GB of RAM. Note the source codes for previous methods, which are written by using Matlab, are available on their websites and adopted for our experiments without any change. As shown in Table 7, histogram-based approaches, e.g., CLAHE, CVC, and LDR, work very fast even with the high resolution image. LIME also shows the fast operation since it employs various speed-up techniques, e.g., FFT (fast Fourier transform) and quadratic approximation, for implementation. In contrast, NPEA and SRIE take quite a lot of times due to the region-based computation and the complicated optimization process, which seriously make the algorithm slow when the image size increases. Since PPEA conducts the subspace analysis at every pixel position, it also takes some time with the high resolution image. As introduced in the previous Section, the proposed method requires the iterative operation, and it thus runs relatively slow compared to several fast algorithms. To improve the processing speed, the proposed method is also implemented with the C language, which accelerates the average processing speed up to 5.27sec and 2.38sec for NASA and HDR datasets, respectively. For further improvement, the spectral domain-based implementation [44] can be applied to the adaptive diffusion process of the proposed method.

FIGURE 17. (a) Original input images. Enhancement results by (b) MST [45], (c) CRM [46], (d) LD [47], and (e) the proposed method.

V. CONCLUSION

In this paper, a novel and simple method for low-light image enhancement is proposed. The key idea of the proposed method is to exploit the maximal value obtained from the diffusion process as the illumination component, which greatly complies with the illumination property in the dark. The estimated illumination component is subsequently separated from the scene reflectance according to the Retinex theory and efficiently stretched by global and local adjustment schemes. One important advantage of the proposed method is that the pixel-wise operation for illumination estimation is effective to suppress blurry artifacts while successfully revealing the underlying structure of a given scene. Based on various experimental results, it is thought that the proposed method can be applied to efficiently improve the visual quality of images acquired under various low-light environments.

REFERENCES

[1] S. Nadimi and B. Bhanu, "Physical models for moving shadow and object detection in video," *IEEE Trans. Pattern Anal. Mach. Intell.*, vol. 26, no. 8, pp. 1079–1087, Aug. 2004.

[2] W. Kim, S. Suh, W. Hwang, and J.-J. Han, "SVD Face: Illumination-invariant face representation," *IEEE Signal Process. Lett.*, vol. 21, no. 11, pp. 1336–1340, Nov. 2014.

[3] T. Mouats, N. Aouf, and M. A. Richardson, "A novel image representation via local frequency analysis for illumination invariant stereo matching," *IEEE Trans. Image Process.*, vol. 24, no. 9, pp. 2685–2700, Sep. 2015.

[4] E. Pisano, S. Zong, B. M. Hemminger, M. DeLuca, R. E. Johnston, K. Müller, M. P. Braeuning, and S. M. Pizer, "Contrast limited adaptive histogram equalization image processing to improve the detection of simulated spiculations in dense mammograms," *J. Digit. Imag.*, vol. 11, no. 4, pp. 193–200, Nov. 1998.

[5] J.-H. Han, S. Yang, and B.-U. Lee, "A novel 3-D color histogram equalization method with uniform 1-D gray scale histogram," *IEEE Trans. Image Process.*, vol. 20, no. 2, pp. 506–512, Feb. 2011.
[6] E. H. Land, "The Retinex theory of color vision," *Sci. Amer.*, vol. 237, no. 6, pp. 108–128, Dec. 1977.
[7] K. He, J. Sun, and X. Tang, "Single image haze removal using dark channel prior," *IEEE Trans. Pattern Anal. Mach. Intell.*, vol. 33, no. 12, pp. 2341–2353, Dec. 2011.
[8] X. Dong, G. Wang, Y. Pang, W. Li, J. Wen. W. Meng, and Y. Lu, "Fast efficient algorithm for enhancement of low lighting video," in *Proc. IEEE Int. Conf. Multimedia Expo*, Jul. 2011, pp. 1–6.
[9] H. Yue, J. Yang, X. Sun, F. Wu, and C. Hou, "Contrast enhancement based on intrinsic image decomposition," *IEEE Trans. Image Process.*, vol. 26, no. 8, pp. 3981–3994, Aug. 2017.
[10] W. Kim, "Image enhancement using patch-based principal energy analysis," *IEEE Access*, vol. 6, pp. 72620–72628, 2018.
[11] B. Funt and L. Shi, "The rehabilitation of MaxRGB," in *Proc. Color Imag. Conf.*, Nov. 2010, pp. 256–259.
[12] R. C. Gonzalez and R. E. Woods, *Digital Image Processing*, 2nd ed. Upper Saddle River, NJ, USA: Prentice-Hall, 2002.
[13] H. Sellahewa and S. A. Jassim, "Image-quality-based adaptive face recognition," *IEEE Trans. Instrum. Meas.*, vol. 59, no. 4, pp. 805–813, Apr. 2010.
[14] A. M. Reza, "Realization of the contrast limited adaptive histogram equalization (CLAHE) for real-time image enhancement," *J. VLSI Signal Process. Syst. Signal, Image Video Technol.*, vol. 38, no. 1, pp. 35–44, 2004.
[15] T. Arici, S. Dikbas, and Y. Altunbasak, "A histogram modification framework and its application for image contrast enhancement," *IEEE Trans. Image Process.*, vol. 18, no. 9, pp. 1921–1935, Sep. 2009.
[16] T. Celik and T. Tjahjadi, "Contextual and variational contrast enhancement," *IEEE Trans. Image Process.*, vol. 20, no. 12, pp. 3431–3441, Dec. 2011.
[17] C. Lee, C. Lee, and C.-S. Kim, "Contrast enhancement based on layered difference representation of 2D histograms," *IEEE Trans. Image Process.*, vol. 22, no. 12, pp. 5372–5384, Dec. 2013.
[18] G. Raju and M. S. Nair, "A fast and efficient color image enhancement method based on fuzzy-logic and histogram," *Int. J. Electron. Commun.*, vol. 68, no. 3, pp. 237–243, Mar. 2014.
[19] K. Gu, G. Zhai, W. Lin, and M. Liu, "The analysis of image contrast: From quality assessment to automatic enhancement," *IEEE Trans. Cybern.*, vol. 46, no. 1, pp. 284–297, Jan. 2016.
[20] D. J. Jobson, Z.-U. Rahman, and G. A. Woodell, "Properties and performance of a center/surround retinex," *IEEE Trans. Image Process.*, vol. 6, no. 3, pp. 451–462, Mar. 1997.
[21] D. J. Jobson, Z.-U. Rahman, and G. A. Woodell, "A multiscale Retinex for bridging the gap between color images and the human observation of scenes," *IEEE Trans. Image Process.*, vol. 6, no. 7, pp. 965–976, Jul. 1997.
[22] J. H. Jang, Y. Bae, and J. B. Ra, "Contrast-enhanced fusion of multisensor images using subband-decomposed multiscale retinex," *IEEE Trans. Image Process.*, vol. 21, no. 8, pp. 3479–3490, Aug. 2012.
[23] K. Xu and C. Jung, "Retinex-based perceptual contrast enhancement in images using luminance adaptation," in *Proc. IEEE Int. Conf. Acoust., Speech Signal Process. (ICASSP)*, Mar. 2017, pp. 1363–1367.
[24] S. Wang, J. Zheng, H.-M. Hu, and B. Li, "Naturalness preserved enhancement algorithm for non-uniform illumination images," *IEEE Trans. Image Process.*, vol. 22, no. 9, pp. 3538–3548, Sep. 2013.
[25] X. Fu, D. Zeng, Y. Huang, Y. Liao, X. Ding, and J. Paisley, "A fusion-based enhancing method for weakly illuminated images," *Signal Process.*, vol. 129, pp. 82–96, Dec. 2016.
[26] X. Fu, D. Zeng, Y. Huang, X.-P. Zhang, and X. Ding, "A weighted variational model for simultaneous reflectance and illumination estimation," in *Proc. IEEE Conf. Comput. Vis. Pattern Recognit.*, Jun. 2016, pp. 2782–2790.
[27] X. Guo, Y. Li, and H. Ling, "LIME: Low-light image enhancement via illumination map estimation," *IEEE Trans. Image Process.*, vol. 26, no. 2, pp. 982–993, Feb. 2017.
[28] P. Perona and J. Malik, "Scale-space and edge detection using anisotropic diffusion," *IEEE Trans. Pattern Anal. Nach. Intell.*, vol. 12, no. 7, pp. 629–639, Jul. 1990.
[29] Y.-L. You, W. Xu, A. Tannenbaum, and M. Kaveh, "Behavioral analysis of anisotropic diffusion in image processing," *IEEE Trans. Image Process.*, vol. 5, no. 11, pp. 1539–1553, Nov. 1996.
[30] J. Weickert, "A review of nonlinear diffusion filtering," in *Scale-Space Theory in Computer Vision*, B. T. H. Romeny, L. Florack, J. Koenderink, and M. Viergever, Eds. Berlin, Germany: Springer, 1997, pp. 3–28.
[31] F. Andreu, V. Caselles, J. I. Diaz, and J. M. Mazón, "Some qualitative properties for the total variation flow," *J. Funct. Anal.*, vol. 188, no. 2, pp. 516–547, Feb. 2002.
[32] M. Rousson, T. Brox, and R. Deriche, "Active unsupervised texture segmentation on a diffusion based feature space," in *Proc. IEEE Comput. Soc. Conf. Comput. Vis. Pattern Recognit.*, Jun. 2003, pp. 699–704.
[33] J. Weickert, B. M. T. H. Romeny, and M. A. Viergever, "Efficient and reliable schemes for nonlinear diffusion filtering," *IEEE Trans. Image Process.*, vol. 7, no. 3, pp. 398–410, Mar. 1998.
[34] *Retinex Theory of Color Vision*, NASA, Washington, DC, USA, 2001.
[35] P. Sen, N. K. Kalantari, M. Yaesoubi, S. Darabi, D. B. Goldman, and E. Shechtman, "Robust patch-based HDR reconstruction of dynamic scenes," *ACM Trans. Graph.*, vol. 31, no. 6, 2012, Art. no. 203.
[36] Q. Wang, X. Fu, X.-P. Zhang, and X. Ding, "A fusion-based method for single backlit image enhancement," in *Proc. IEEE Int. Conf. Image Process. (ICIP)*, Sep. 2016, pp. 4077–4081.
[37] A. Mittal, R. Soundararajan, and A. C. Bovik, "Making a "completely blind" image quality analyzer," *IEEE Signal Process. Lett.*, vol. 20, no. 3, pp. 209–212, Mar. 2013.
[38] K. Gu, S. Wang, G. Zhai, S. Ma, X. Yang, W. Lin, W. Zhang, and W. Gao, "Blind quality assessment of tone-mapped images via analysis of information, naturalness, and structure," *IEEE Trans. Multimedia*, vol. 18, no. 3, pp. 432–443, Mar. 2016.
[39] K. Gu, W. Lin, G. Zhai, X. Yang, W. Zhang, and C. W. Chen, "No-reference quality metric of contrast-distorted images based on information maximization," *IEEE Trans. Cybern.*, vol. 47, no. 12, pp. 4559–4565, Dec. 2017.
[40] K. Gu, D. Tao, J.-F. Qiao, and W. Lin, "Learning a no-reference quality assessment model of enhanced images with big data," *IEEE Trans. Neural Netw. Learn. Syst.*, vol. 29, no. 4, pp. 1301–1313, Apr. 2018.
[41] *ISO12640-2*. Accessed: Jul. 22, 2019. [Online]. Available: http://www.iso.org/
[42] *Canon*. Accessed: Jul. 22, 2019. [Online]. Available: http://www.cipr.rpi.edu/resource/stills/canon.html/
[43] *Kodak Lossless True Color Image Suite*. Accessed: Jul. 22, 2019. [Online]. Available: http://r0k.us/graphics/kodak/
[44] J. M. Morel, A. B. Petro, and C. Sbert, "A PDE formalization of retinex theory," *IEEE Trans. Image Process.*, vol. 19, no. 11, pp. 2825–2837, Nov. 2010.
[45] Z. Farbman, R. Fattal, D. Lischinski, and R. Szeliski, "Edge-preserving decompositions for multi-scale tone and detail manipulation," *ACM Trans. Graph.*, vol. 27, no. 3, Aug. 2008, Art. no. 67.
[46] Z. Ying, G. Li, Y. Ren, R. Wang, and W. Wang, "A new low-light image enhancement algorithm using camera response model," in *Proc. IEEE Int. Conf. Comput. Vis. Workshop (ICCVW)*, Oct. 2017, pp. 3015–3022.
[47] Z. Liang, J. Xu, D. Zhang, Z. Cao, and L. Zhang, "A hybrid l_1-l_0 layer decomposition model for tone mapping," in *Proc. IEEE Int. Conf. Comput. Vis., Pattern Recognit.*, Jun. 2018, pp. 4758–4766.

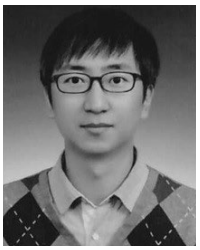

WONJUN KIM (M'13) received the B.S. degree from the Department of Electronic Engineering, Sogang University, Seoul, South Korea, in 2006, the M.S. degree from the Department of Information and Communications, Korea Advanced Institute of Science and Technology (KAIST), Daejeon, South Korea, in 2008, and the Ph.D. degree from the Department of Electrical Engineering, KAIST, in 2012. From September 2012 to February 2016, he was a Research Staff Member with the Samsung Advanced Institute of Technology (SAIT), South Korea. Since March 2016, he has been with the Department of Electronics Engineering, Konkuk University, Seoul, where he is currently an Assistant Professor. His research interests include image and video understanding, computer vision, pattern recognition, and biometrics, with an emphasis on background subtraction, saliency detection, and face and action recognition. He has served as a Regular Reviewer for over 30 international journal articles, including the IEEE TRANSACTIONS ON IMAGE PROCESSING, IEEE ACCESS, IEEE TRANSACTIONS ON CIRCUITS AND SYSTEMS FOR VIDEO TECHNOLOGY, IEEE TRANSACTIONS ON MULTIMEDIA, IEEE TRANSACTIONS ON CYBERNETICS, IEEE SIGNAL PROCESSING LETTERS, and *Pattern Recognition*.

RYONG LEE received the B.S. degree from the School of Electronics, Telecommunication and Computer Engineering, Korea Aerospace University, South Korea, in 1998, and the M.S. and Ph.D. degrees from the Department of Social Informatics, Kyoto University, Japan, in 2001 and 2003, respectively. From 2003 to 2008, he was a Research Staff Member with the Samsung Advanced Institute of Technology (SAIT), South Korea. Since 2013, he has been with the Korea Institute of Science and Technology Information (KISTI), South Korea, where he is currently a Senior Researcher with Research Data Sharing Center. His research interests include spatial data analysis, the Internet of Things, smart city, and artificial intelligence.

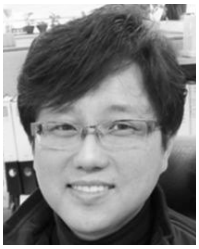

MINWOO PARK received the B.S. and M.S. degrees from the Division of Computer Convergence, Chungnam National University, South Korea, in 1992 and 2004, respectively. Since 1996, he has been with the Korea Institute of Science and Technology Information (KISTI), South Korea, where he is currently the Team Manager of Research Data Sharing Center. His research interests include system architecture, information security, the Internet of Things, smart city, and artificial intelligence.

SANG-HWAN LEE received the B.S. degree from the Department of Electronic Computing, University of Ulsan, South Korea, in 1992, the M.S. degree in software engineering from Korea University, in 2004, and the Ph.D. degree from the Department of Computer Science, University of Seoul, South Korea, in 2018. Since 1995, he has been with the Korea Institute of Science and Technology Information (KISTI), South Korea, where he is currently the Director of Research Data Sharing Center. His research interests include big data analysis, large research data, data governance, data ecosystems, and artificial intelligence.